BLIND PREDICTION OF A 7-STOREY RC FRAME WITH DIFFERENT SOURCES OF TORSIONAL IRREGULARITY

A. Kagermanov[1], I. Markovic[2]

[1] *Research Associate, University of Applied Science Rapperswil, alexander.kagermanov@hsr.ch*
[2] *Professor, University of Applied Science Rapperswil, ivan.markovic@hsr.ch*
...

Abstract

Numerical analyses performed as part of the QuakeCoRE-NCREE Blind Prediction Competition 2019 are presented. Two specimens with different sources of torsional irregularity were tested on the shaking table under increasing level of unidirectional excitation. The specimens consisted of 7-storey RC frames with perimeter RC shear walls in the short direction between stories 2 and 7, thus creating a soft-storey configuration at the ground level. Torsional irregularity in specimen-1 was introduced with an URM infill built on the west side of the soft-storey. Specimen-1 was retested after removing the URM infill and without any repair, in order to investigate the effect of damage irregularity. Specimen-2 was similar to specimen-1, however there was no URM infill. Torsional irregularity was introduced by decreasing the amount of transverse reinforcement in the columns located on the east side and middle frames of the soft-storey. Preliminary analyses suggested that torsional response would be triggered after buckling of longitudinal reinforcement in the plastic hinge regions. The paper presents the modeling approach and results submitted by the author in the category of nonlinear time-history analysis. Published results submitted by other participants are summarized as well. It can be said that overall none of the predictions reflected with sufficient accuracy the experimentally observed behavior. Causes and considerations for model improvement are discussed at the end of the paper.

Keywords: blind prediction, rc frame, nonlinear time history, torsional irregularity, reinforcement buckling

1. Introduction

An international blind prediction contest has been recently organized by the National Center for Earthquake Engineering (NCREE) and QuakeCoRE on the dynamic response of RC buildings with torsional eccentricity [1]. The specimens were designed based on the structural systems of two RC residential buildings that collapsed during the 2016 Meinong Earthquake in Tainan. Two categories were considered: (a) nonlinear time-history analysis (NLTHA) and (b) all other methods. Fourteen predictions were submitted in category (a) and two in category (b). Participants were asked to predict the 1st and roof storey displacements in the direction of applied ground motion and perpendicular to it, the 1st and roof storey diaphragm rotation, absolute accelerations and the period of the structure before each ground motion input.

The prediction can be regarded as rather challenging, involving the three dimensional dynamic response of a multi-storey building with torsional eccentricity, subjected to different damage scenarios and increasing ground motions. Significant damage was attained during the test reaching a maximum inter-storey drift of 15% and causing residual displacements. The specimens lost, or were very close to, their vertical load carrying capacity [2].

Based on the submissions it can be said that overall none of the predictions reflected with sufficient accuracy the experimentally observed behavior. The modeling approach and results submitted by the author are briefly discussed in the paper. Limited information is currently available on the on-going research project to determine the actual reasons of discrepancy between experiment and predictions. Possible causes and considerations for model improvement are discussed at the end.

2. Experimental test summary

Two half-scale RC specimens were tested under unidirectional excitation in the NCREE earthquake simulator (Fig.1). The specimens presented seven stories, two 3.5m bays in the y (long-direction) and one 3.5m bay in the short (x-direction). RC shear walls were located in the six stories above the ground level, creating a soft-storey configuration. The upper units B and C were intended to be reused for the second specimen, whereas unit A was modified in order to investigate different sources of irregularity. For specimen 1 (SP1-A), an UMR infill wall was placed on the right side of the soft-storey in the x-direction, resulting in stiffness and strength eccentricity. After the first testing sequence, the infill was removed and the specimen was retested (SP1-B) under a similar sequence of ground motions. For specimen 2 (SP2), the transverse reinforcement ratio of the ground floor columns located of the left and middle frames was decreased with respect to specimen 1, resulting in eccentric strength degradation of non-ductile elements.

The applied ground motion corresponded to the 1999 Chi-chi record (CHY101E). The record was scaled by $1/\sqrt{2}$ in time and amplified by a factor of 2.65, giving the 100% test ground motion (Fig.2). This record was applied with increasing ground motion intensity (GMI) for each structure as shown in Table 1.

Table 1 – Ground motion input sequence

	Testing sequence										
	SP1-A				SP1-B				SP2		
Input-GMI	10%	20%	60%	60%-2	10%	20%	40%	60%	10%	20%	40%
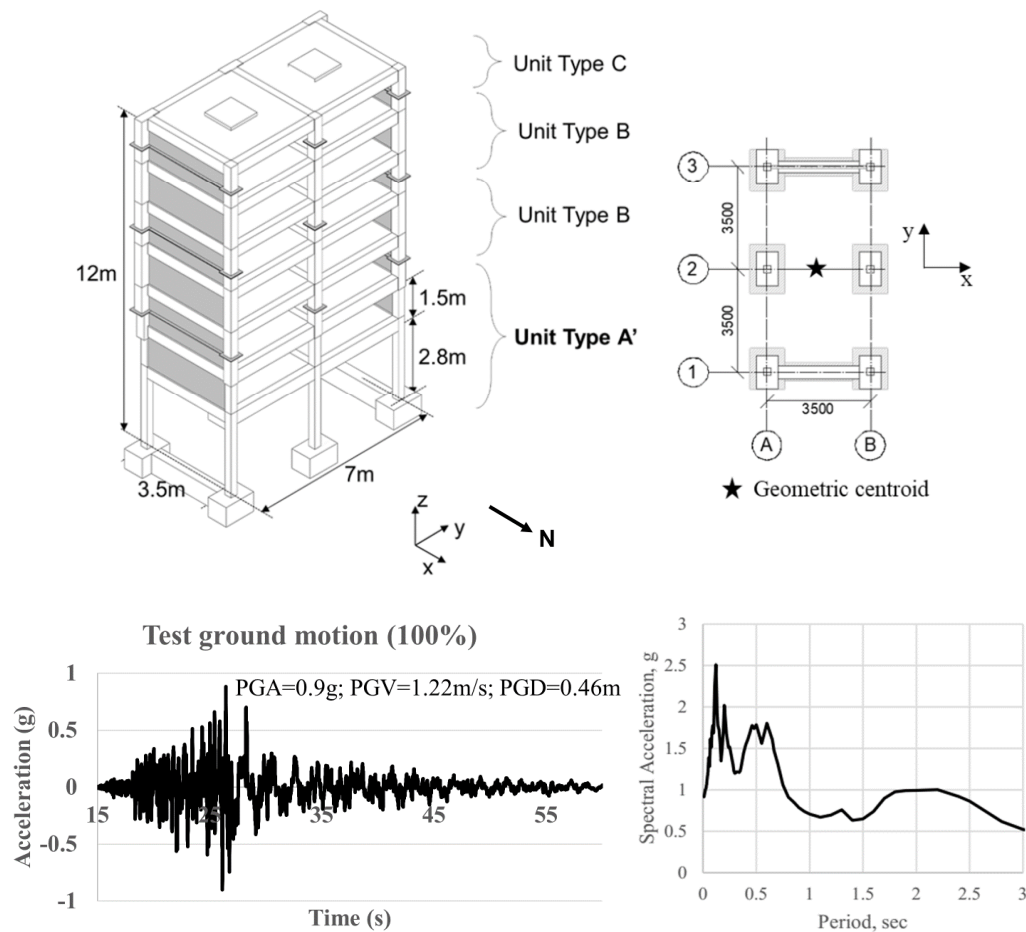
Fig. 1 – Specimen layout, 100% acceleration time history and corresponding response spectrum [1].

3. Blind prediction model

A 3D model of the building was set up using an in-house FE software IDEEA [3, 4, 5, 6, 7]. The model consisted of a combination of inelastic and elastic frame elements to model beams and columns, and elastic and inelastic shell elements to model the shear walls. Elastic elements were used to model modules B and C, which were designed as replaceable elements, whereas inelastic elements were used in module A, which was expected to experience most of the inelastic response.

Inelastic frame elements were displacement-based beam-column elements with mesh refinement in the plastic hinge region. Inelastic wall elements were layered shell elements based on a fixed-smeared-crack constitutive model for cracked concrete. Wall elements were directly connected to the boundary columns and through rigid links to the top and bottom beams. A fiber-section model was used to define the axial-flexural response of the frame elements. The uniaxial response of concrete was modeled based on Mander et al. [8] with refined rules for cyclic strength and stiffness degradation [9]. A confinement factor of 1.2 was used for fibers within the concrete core. Confinement in the poorly detailed columns of specimen 2 was neglected. The critical issue in these columns was expected to be concrete cover spalling and buckling of longitudinal reinforcement. Spalling was not explicitly modeled. Buckling was taken into account based on the modified Menegotto-Pinto model [10, 11].

3

2i-0108

A nearly rigid diaphragm was assumed for the slabs, which was imposed by means of very stiff diagonal tie members connected between beam-column joints. The structure was fully fixed at the base, which was taken at a level slightly below the foundation top face in order to account for strain penetration effects. Joint regions were modeled with elastic frame elements which stiffness was that of the corresponding elements framing into the joint.

The infill panel was modeled with equivalent diagonal struts. The hysteretic rule presented an initial elastic stiffness up to the maximum strength followed by a linear softening branch with a slope equal to 3% of the initial stiffness. The properties of the struts were obtained based on [12]. For specimen 1, which had the infills removed after the first testing sequence, full removal of the strut elements was implemented in the program, hence the whole sequence of eight ground motions was executed in a single run.

Masses were modeled using a lumped mass matrix. The additional concrete blocks were modeled as discrete masses defined in the center of the diagonal ties. With this approach the in-plane rotational inertia of the slab with respect to its geometric center was estimated as 40.4tm^2, which was considered close enough to the exact value of 37.5tm^2. The total mass of the model (107.24t) was slightly lower than the one reported in the experiment (108.9t). P-delta effects were taken into account by defining permanent gravity loads at the beam-column joints.

1% mass and initial stiffness proportional Rayleigh damping was assumed. The analysis was carried out using the Newmark average-acceleration method with a time step of $\Delta t = 0.03\text{s}$. This rather coarse time step was chosen to minimize computational time. Comparison with $\Delta t = 0.01\text{s}$ showed a relatively small difference in terms of displacements. The natural period corresponding to the fundamental mode shape torsion-bending in the short direction using un-cracked member stiffness was 0.55s.
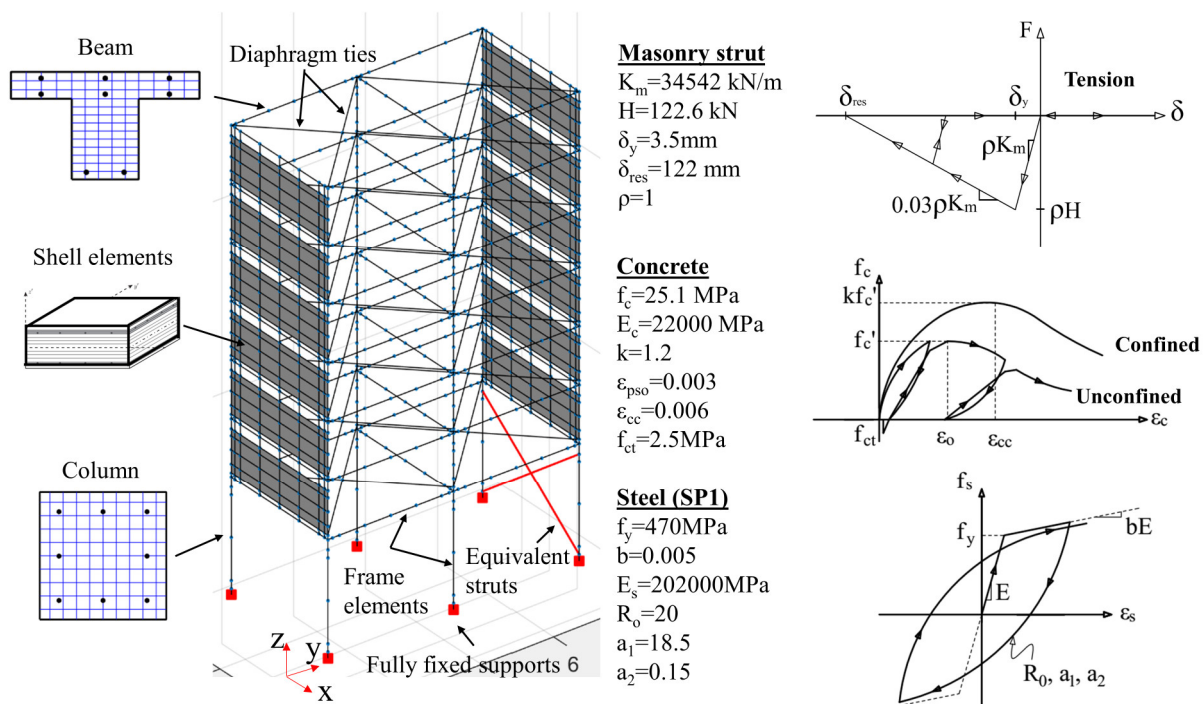
Fig. 2 – Summary of the modelling approach: 3D Numerical model in IDEEA and material parameters.

4. Numerical model performance

Overall the numerical model performed as expected. Most of the displacement demand concentrated at the soft-storey, whereas the upper stories behaved elastically. Plastic hinges formed at all column ends with yielding of longitudinal reinforcement and concrete crushing. In SP1-A, torsional response was first triggered by stiffness eccentricity of the infill, which induced higher damage to the eastern columns. The infill panel reached its maximum capacity at 20% GMI. The maximum value of torsional rotation occurred at 60% GMI, decreasing afterwards. The period elongated from 0.55s at 10% to 0.85s at 60%-2. For SP1-B, torsional response due to pre-existing damage was present, although the maximum displacements and rotations were overall lower than for SP1-A. For SP2, torsional response was triggered during 40% GMI at buckling of longitudinal reinforcement.

Table 2 summarizes some of the numerical values submitted to the contest: (i) the natural period before each input, (ii) the maximum displacement in the x direction at the 1st storey in the eastern frame, (iii) the 1st floor diaphragm rotation and (iv) the maximum displacement in the y direction at the 1st storey. Fig.3 shows the collapse mechanism from the model and the experiment for specimen SP1-B at the end of the test.

Table 2 – Submitted results for period, displacement and diaphragm rotation

	SP1-A				SP1-B				SP2		
Ground motion intesity	10%	20%	60%	60%-2	10%	20%	40%	60%	10%	20%	40%
Period (s)	0.55	0.55	0.65	0.85	0.85	0.95	0.95	0.95	0.56	0.56	0.7
Maximum x displacement at 1st storey (mm)	-12.8	40.1	82.1	83.4	14.8	22.5	46.6	66.1	11.1	34.3	40.9
Diaphragm rotation at 1st storey corresponding to the max. x displacement (mrad)	-1.64	5.19	10.34	5.01	0.47	0.45	2.32	3.47	-0.04	-0.04	0.14
Maximum y displacement at 1st storey (mm)	-3.36	-9.95	18.71	-12.43	-1.03	-2.10	-4.74	-6.74	0.14	-0.46	-1.39

■ Concrete crushing   ★ Concrete crushing and steel yielding
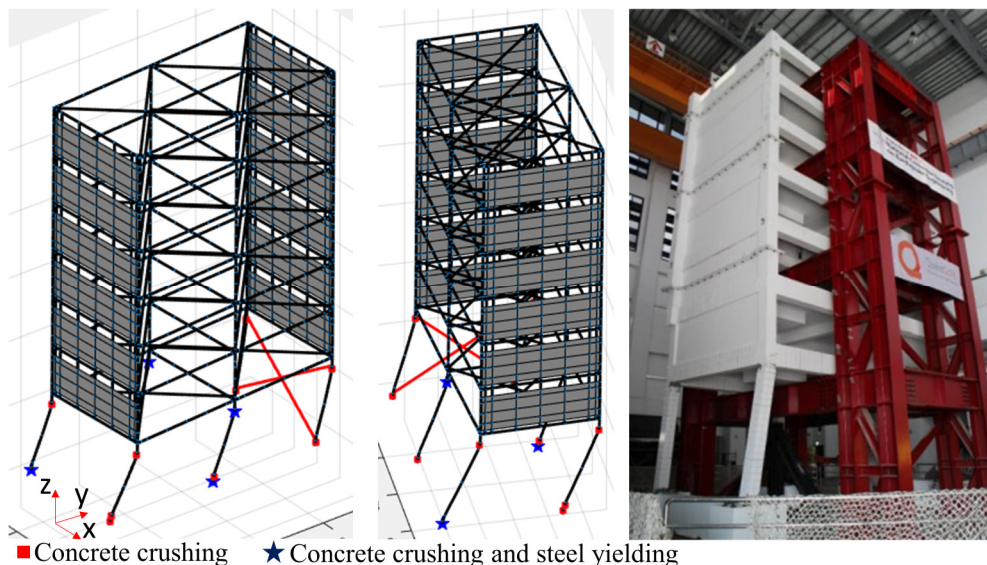
Fig. 3 – Calculated collapse mechanism and the experimentally observed one for Specimen SP-1-B [2]

5

5. Blind prediction results

The figures below summarize results from the blind prediction including the range of submitted predictions, the author's prediction and some "post-diction" results considering the flexibility of the foundation discussed in the next section. The response quantities correspond to those in table 2: maximum displacement in the x direction of the eastern frame, diaphragm rotation and the maximum displacement in the y direction. Results regarding absolute accelerations can be found elsewhere [2].
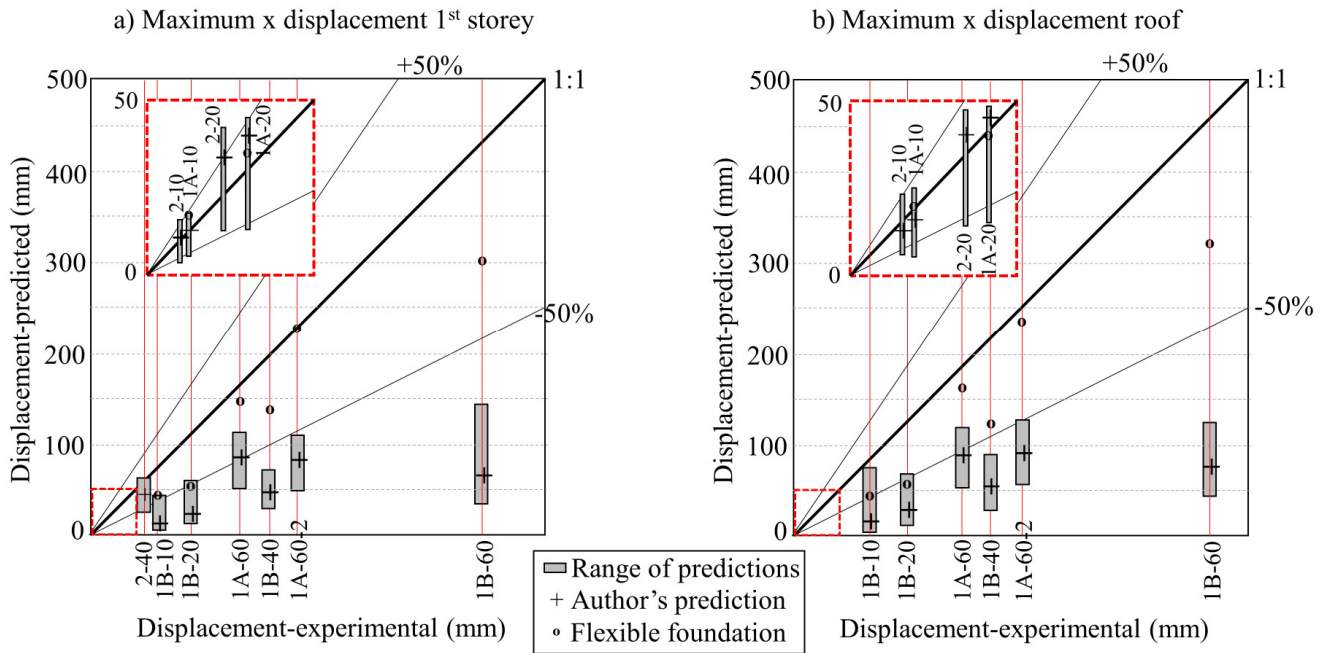
Fig. 4 – Maximum x displacement at 1st storey and roof.
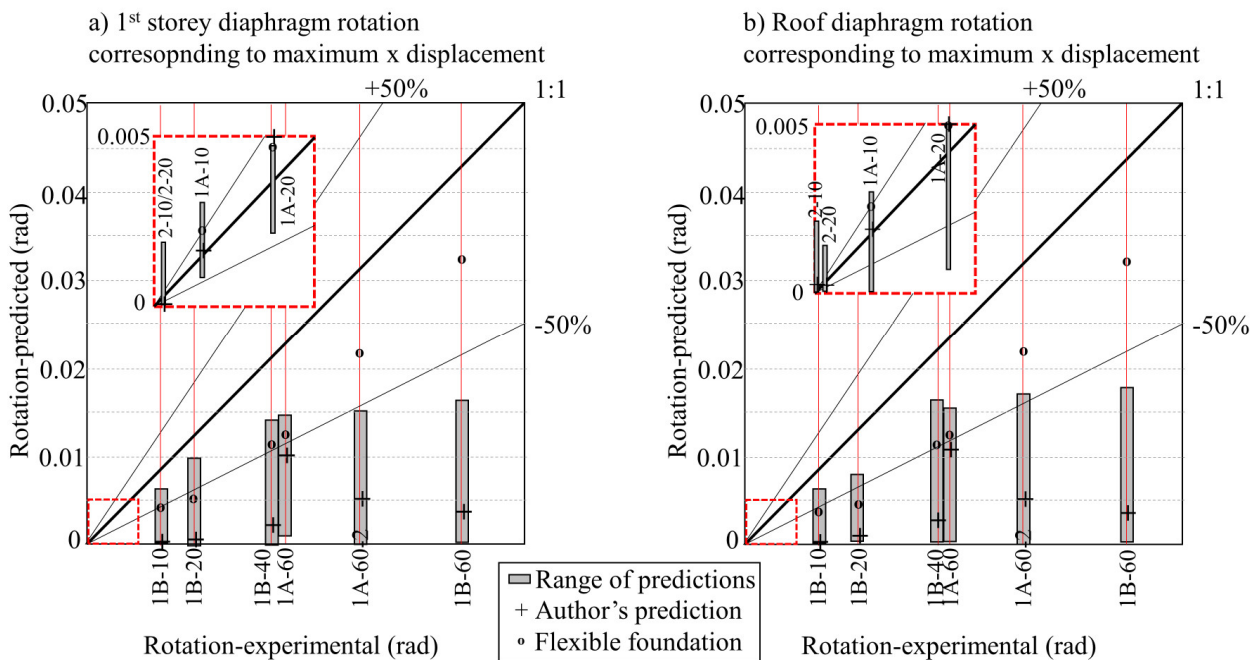
Fig. 5 – Maximum diaphragm rotation at 1st storey and roof.

6
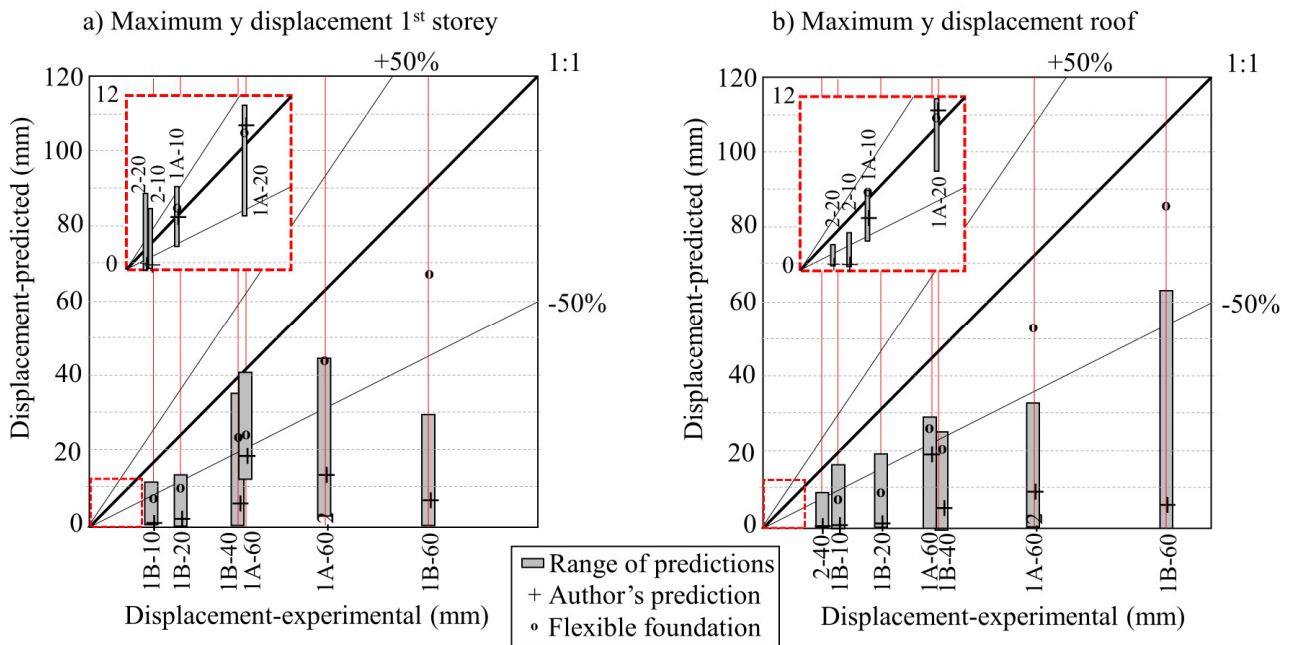
Fig. 6 – Maximum y displacement at 1st storey and roof.

The following observations can be made:

-Significantly higher displacements and rotations were reached in the experiment compared to the predictions, especially at large GMI levels. The maximum x displacement reached 450mm, whereas the numerical predictions scattered around 100mm.

-There was evident damage accumulation and cyclic degradation due to repeated shaking resulting in substantial displacement amplification. Numerical predictions were unable to capture these effects. Note for instance that the range of predictions for 1A-60% and 1A-60%-2 remains essentially the same, whereas in the experiment an increase of 40% is observed

-It is likely that specimen 1-A was more affected by damage accumulation and period elongation, whereas specimen 1-B by residual displacements.

-By comparing the 1st storey displacements against the roof displacements an idea of the behavior of the upper stories can be obtained. Usually displacements in the x and y directions amplify (y displacement more due to the frame flexibility), whereas the diaphragm rotations remain constant. This is due to the fact that torsional eccentricity is only present at the 1st storey. Upper stories are symmetric in plan with respect to the x axis, thus their response is mainly in bending.

-Diaphragm rotation and transverse displacement for specimen 2 are very small, suggesting that eccentricity caused by asymmetric transverse reinforcement does not induce torsion for the given GMI. Damage pictures reported in [2] suggest that axial-shear failure occurred in the columns. As discussed later, significant tensile forces may have been induced in the columns during the test.

-The eccentric infill induces significant torsion (compare diaphragm rotation of specimen 1 and 2). The largest rotation however is due to damage irregularity in specimen 1-B. Its amplification with increasing GMI is also more accentuated.

-Comparison with numerical results suggests the existence of a critical damage eccentricity threshold after which significant displacement amplification and system instability increases with repeated ground shaking.

7

6. Possible causes and model improvement

Based on the above it can be said that overall numerical models performed stiffer, predicted less damage and were unable to capture displacement amplification effects due to repeated ground motion. However, the models were relatively consistent between each other suggesting that something was generally missed by the participants.

The experimental period before any input was 0.93s for specimen 2 and 0.89s for specimen 1-A which reflects the range of initial mass and stiffness as well as the effect of infills. The numerical models predicted an initial period of 0.55s on average [2]. Even accounting for pre-cracking of the specimen (due to shrinkage, transportation, manipulation, white noise testing, etc…) does not explain the observed flexibility.

A possible reason considered here is the influence of the foundation, which was likely assumed as infinitely stiff by the participants. The actual foundation consisted of concrete pedestals and tie beams present only in the perimeter frames in the short (x) direction and attached with D22 shear studs and M20 bolts to the shaking table (Fig.7). Moreover, peak horizontal accelerations of 0.4g were recorded during the shaking, which can induce significant overturning moments. The corresponding uplifting reactions at column bases are in the order of 500kN, which is about twice the reaction due to gravity loads. This combined with horizontal forces due to bending and torsion could potentially engage some level of uplifting, sliding and rotation of the foundation.

Simple modifications of the boundary conditions were introduced accounting for foundation flexibility and possible cracking (Fig.7): (i) the tie beams were modeled with inelastic fiber-elements, (ii) the three translational degrees of freedom in the center of tie beams and intermediate column supports were restrained, and (iii) the vertical translation of the corner columns was restrained. The natural period with uncracked stiffnesses was 0.60s. The results obtained with this model for SP1-A and SP1-B were summarized in Figures 4-6. A clear improvement can be observed especially regarding damage accumulation and displacement amplification at large GMI levels, although maximum values are still underestimated. Note that this rather simple approach is only an approximation to the complex foundation response.
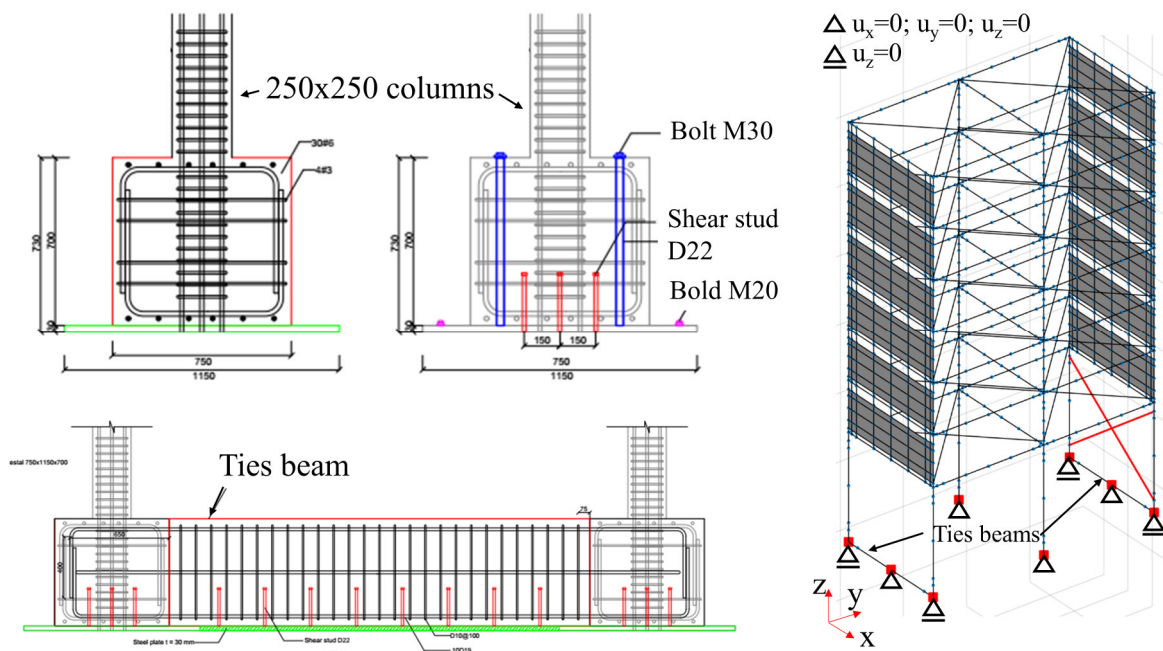
Fig. 7 – Foundation layout and model modification of boundary conditions [1].

7. Conclusions

Results from the recent blind prediction on a multi-storey RC frame building with torsional eccentricity could not reproduce with sufficient accuracy the experimentally observed behavior. The actual response showed significantly higher displacements and rotations, as well as damage accumulation and displacement amplification with repeated ground excitation. The deviation between predictions and experiment increased with increasing ground motion intensity. However most of the predictions were relatively close among each other, at least in terms of the less challenging response parameters such as maximum displacements, suggesting that the state-of-the-knowledge in nonlinear time-history analysis was consistently applied, but also that something was generally missed by the participants which did happen in the experiment. The initial period of the structure measured before any input was almost twice the submitted average value, meaning that the specimens were already much more flexible from the beginning. The actual reason for this should be clarified in the future as additional experimental data from the on-going project becomes available. In the paper the influence of foundation flexibility and boundary conditions was considered as a possible reason. Simple modifications were introduced in the existing model allowing flexural deformation and rigid body motion of tie beams. Despite a clear improvement, maximum displacements and diaphragm rotations were still underestimated.

8. References

[1] QuakeCoRE-NCREE Blind Prediction Competition 2019. Supporting Documentation. Description of Tests. *https://www.quakecore.nz/blind-prediction-competition-2019*

[2] QuakeCoRE-NCREE Blind Prediction Competition 2019. Results. *https://www.quakecore.nz/blind-prediction-competition-2019-results*

[3] IDEEA3D: Nonlinear FEA Software, 2018. Available at: https://sites.google.com/site/ideeanalysis/

[4] Kagermanov, A, Ceresa, P. [2017] "Modelling Flexure-Shear Failures in Masonry-Infilled RC frames with Inelastic Fiber-based Frame Elements" Proceedings of COMPDYN 2017 and 6th ECCOMAS *Thematic Conference of Computational Methods in Structural Dynamics and Earthquake Engineering*, Rodhes I, June 15-17, Greece.

[5] Kagermanov, A., and Ceresa, P. (2016). "Physically Based Cyclic Tensile Model for RC Membrane Elements." *Journal of Structural Engineering* (ASCE), Vol.142, Issue 12, December.

[6] Kagermanov, A., Ceresa, P., (2017) "Fiber-section model with an exact shear strain distribution for RC frame elements". *Journal of Structural Engineering*, (ASCE), Vol.143, Issue 10, October.

[7] Kagermanov, A., Ceresa, P., (2018) "3D fiber-based frame element with multiaxial stress interaction for RC structures". *Advances in Civil Engineering*, Vol. (5):1-13

[8] Mander, J.B., Priestley, M.J.N., Park, R. [1988] "Theoretical stress–strain model for confined concrete". *J. Struct Eng.* 114(8):1804–1826

[9] Martinez-Rueda, J.E., Elnashai, A.S. [1997] "Confined concrete model under cyclic load," *Materials and Structures* 30(197),139-147.

[10] Menegotto, M., Pinto, P.E. [1973] "Method of analysis of cyclically loaded reinforced concrete plane frames including changes in geometry and non-elastic behavior of elements under combined normal force and bending." *IABSE symposium, resistance and ultimate deformability of structures acted on by well-defined repeated loads*, IABSE, Zurich, Switzerland

[11] Monti, G., Nuti, C. [1992] "Nonlinear cyclic behavior of reinforcing bars including buckling" *Journal of Structural Engineering,* Vol. 118, No. 12, December.

[12] Decanini, L., Mollaioli, F., Mura, A., Saragoni, R. [2004] "Seismic performance of masonry infilled RC frames" *13th World Conference on Earthquake Engineering*, Vancouver, Canada